Sensors & Transducers, Vol. 160, Issue 12, December 2013, pp. 563-569

www.sensorsportal.com

Sensors & Transducers

© 2013 by IFSA

http://www.sensorsportal.com

Chassis Integrated Control for Electric Vehicle with Four In-Wheel Motors

[1,2] Gang LI, [2] Chang-Fu ZONG, [1] Shi JING, [1] Zhi-Cheng Zhou, [1] Hang YUAN

[1] Liaoning University of Technology,
Jinzhou Liaoning, 121001, China
[2] State Key Laboratory of Automotive Simulation and Control, Jilin University,
Changchun, 130025, China
Tel.:+86-13614162583, fax: +86-04164199435
E-mail: lnitligang@126.com

Received: 8 October 2013 /Accepted: 22 November 2013 /Published: 30 December 2013

Abstract: With the development of the in-wheel motor technology, driving, braking and active suspension are integrated in single in-wheel motor. It is easier to achieve the integrated control for in-wheel motor electric vehicle through X-by-wire technology. For enhancing the vehicle handling and stability, the integrated control of active steering (AFS), direct yaw moment (DYC) and active suspension (AS) is studied in this paper. The integrated algorithm adopts hierarchical integrated control structure. The model predictive controller is designed. The driving torque control allocation rules and active suspension control methods are studied. It achieves integrated control of AFS/DYC and integrated control of AFS/DYC/AS. The simulation test is used to verify the algorithm. The result shows that the algorithm can make the vehicle follow the desired values effectively and enhance the vehicle stability and active safety in extreme conditions. *Copyright © 2013 IFSA.*

Keywords: In-wheel motor, Electric vehicle, Integrated control, X-by-wire technology, Active steering, Direct yaw moment, Active suspension.

1. Introduction

Under the pressure of energy conservation and environmental protection, various forms of electric vehicles are becoming the focus of the world auto industry R & D and four in-wheel motor electric vehicle has become the more promising one. With the development of the in-wheel motor technology, driving, braking and active suspension are integrated in single in-wheel motor. It is easier to achieve the integrated control for in-wheel motor electric vehicle through X-by-wire technology. Four in-wheel motor electric vehicle is easy to achieve direct yaw moment control (DYC) through controlling motor torque. In-wheel motors can generate driving torque quickly, accurately and independently. There was some research on four-wheel independently driven electric vehicle DYC in recent years [4-6]. Vehicle active front steering (AFS) generates compensated yaw moment to ensure the stability of the vehicle by active steer angle to changing the tires' lateral forces [7]. AFS is weaker in stability control than DYC, but it has certain advantages compare to the DYC in ride comfort. It is very good to play the respective advantages and eliminate the interference when the AFS and DYC are all in the vehicle. AFS/DYC

integrated control of four in-wheel motor electric vehicle has become one of the important integrated chassis control research [8-9]. Active suspension (AS) can improve the vehicle ride comfort and handling stability better in different driving conditions compare to the traditional suspension system. When the vehicle has AFS, DYC, AS and other control subsystems, it must coordinate the mutual interferences between the various subsystems. The integrated control of the vehicle chassis has become the study hotspot for developing the vehicle performance potential.

In the view of improving vehicle handling and stability, AFS/DYC/AS integrated control algorithm of four in-wheel motor electric vehicle is studied in this paper. The hierarchical integrated control structure is adopted in this paper. The model predictive controller, the driving force allocation controller and the active suspension controller are designed. The algorithm is verified by simulation based on the multi-degree of freedom vehicle simulation model.

2. Vehicle Model

The 14-DOF nonlinear vehicle model is established by the Matlab/Simulink in this paper. It includes 6-DOF of body translation and rotation, 4-DOF of unsprung mass vertical movement and 4-DOF of wheel rotation. The transient Magic-formula tire model is used in the vehicle model. Because the modern motor controller is mature, motor response speed is dozens times of the speed of the vehicle response, so the model does not pay attention to the motor control system performance. This paper focuses on the effectiveness of integrated control algorithm and the motor model is simplified as the driving torque input with the first-order lag characteristics. The vehicle model can reflect the vehicle dynamic characteristics, which is easy to add control algorithms and make evaluation. Table 1 shows part of the vehicle model parameters.

Table 1. Part of the vehicle model parameters table.

Parameter	Value
Vehicle mass m /kg	827
Height of CG h /m	0.45
Distance between CG and front axle a /m	1.110
Distance between CG and rear axle b /m	1.25
Inertia moment I_z /kg.m2	1210
Front axle cornering stiffness k_1 / N.rad-1	-1.33×10^5
Rear axle cornering stiffness k_2 / N.rad-1	-1.21×10^5

The hierarchical integrated control structure is adopted in this algorithm as shown in Fig. 1. It includes signal processing layer, integrated control layer, control allocation layer and execution layer. The driver maneuvering signal and the vehicle speed signal are processed in the signal processing layer. According to the driver maneuvering signal and the vehicle velocity signal, the vehicle desired yaw rate, desired slip angle and the target vehicle speed are calculated based on the reference model. The 2-DOF linear vehicle model is used as the reference model. The desired slip angle boundary and yaw rate boundary can be expressed as follows [13]:

$$|\gamma_d| \le 0.85\frac{\mu g}{V_x},\ |\beta_d| \le \tan^{-1}(0.02\mu g), \tag{1}$$

where μ is the road surface friction coefficient.

According to the signal processing layer, the active steer angle $\Delta\delta_f$, the yaw moment ΔM and the desired total driving torque T_{xrep} are calculated in the integrated control layer by optimizing. The active steer angle is directly to the bottom actuator and the yaw moment is achieved by the driving force allocation. To improve the stability of the vehicle in severe conditions, suspension integration adopts logic integrated control in this paper. When the lateral acceleration exceeds certain limits, the active suspension control starts. The integrated control algorithm is mainly studied in this paper and assumes that the vehicle state is known. The vehicle state estimation can reference the paper [14].

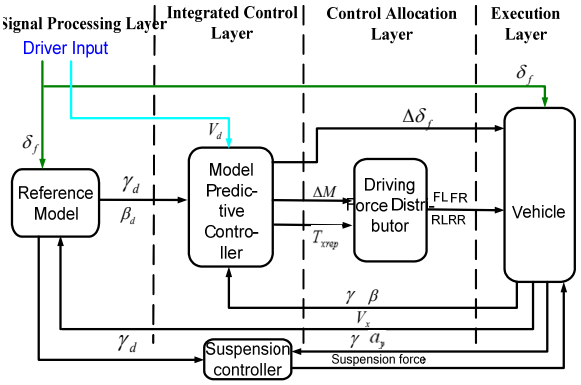

Fig. 1. Hierarchical integrated control structure.

3. Controller Design

The model predictive controller based on the model predictive theory, the driving force allocation controller and the active suspension controller are designed.

3.1. Model Predictive Controller Design

The model predictive control includes the prediction model, rolling optimization and feedback correction [15].

For the purpose of real-time control, the 2-DOF vehicle model with the yaw moment is adopted as the prediction model in this paper. The state space can be expressed as follows:

$$\begin{aligned} \dot{x}(t) &= A_c x(t) + B_c u(t) \\ y_c(t) &= C_c x(t) \end{aligned}, \tag{2}$$

where

$$A_c = \begin{bmatrix} \frac{k_1 + k_2}{mV_x} & \frac{ak_1 - bk_2}{mV_x^2} - 1 \\ \frac{ak_1 - bk_2}{I_z} & \frac{a^2 k_1 + b^2 k_2}{I_z V_x} \end{bmatrix}, \quad B_c = \begin{bmatrix} \frac{-k_1}{mV_x} & 0 \\ \frac{-ak_1}{I_z} & \frac{1}{I_z} \end{bmatrix},$$

$$C_c = \begin{bmatrix} 1 & 0 \\ 0 & 1 \end{bmatrix}, \quad x(t) = \begin{bmatrix} \beta \\ r \end{bmatrix}, \quad u(t) = \begin{bmatrix} \delta_f \\ \mathrm{M} \end{bmatrix}.$$

where k_1 is the front axle cornering stiffness; k_2 is the rear axle cornering stiffness; I_z is the inertia moment about yaw axis; δ_f is the steer angle of front wheel; M is the yaw moment.

The 2-DOF vehicle model uses the two line-type tire model for solving the problem of the stability control limitations as shown in Fig. 2. The 2-DOF vehicle model axle cornering stiffness is considered to be in the linear region when the tires don't reach saturation. The cornering stiffness is set to 0 when the tires are saturated.

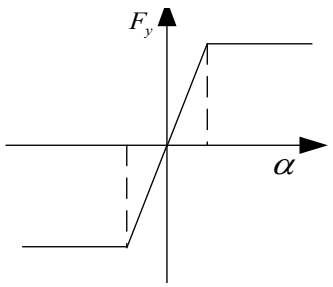

Fig. 2. Two line-type tire model.

Model predictive control is discrete control and the discrete formula (2) can be expressed as follows:

$$\begin{aligned} \Delta x(k+1) &= A\Delta x(k) + B\Delta u(k) \\ y_c(k) &= \Delta x(k) + y_c(k-1) \end{aligned}, \tag{3}$$

where

$$\Delta x(k) = x(k) - x(k-1)$$
$$\Delta u(k) = u(k) - u(k-1)$$

$$\Delta x = \begin{bmatrix} \Delta\beta \\ \Delta r \end{bmatrix}, \quad \Delta u = \begin{bmatrix} \Delta\delta_f \\ \Delta\mathrm{M} \end{bmatrix}$$

A, B, C are discrete matrices. Based on the model predictive control theory, the initial conditions are the latest measurements. Dynamic prediction of future process is done based on prediction model. Prediction time domain is set as p .Control time domain is set as m . Set $m < p$. $m = 2$ and $p = 10$ in this paper. The k moment for $k+i$ moment state prediction is defined as $x(k+i \mid k)$. $\Delta u(k+i)$ is control increment. $y_c(k+i \mid k)$ is output. Out of control time domain $\Delta u(k+i) = 0, i \geq m$.

Define vectors:

$$Y_p(k+1 \mid k) = \begin{bmatrix} y_c(k+1 \mid k) & y_c(k+2 \mid k) & \ldots & y_c(k+p \mid k) \end{bmatrix}^T \tag{4}$$

$$\Delta U(k) = \begin{bmatrix} \Delta u(k) & \Delta u(k+1) & \ldots & \Delta u(k+m-1) \end{bmatrix}^{\mathrm{T}} \tag{5}$$

The system future p step prediction output can be calculated by the follow equation:

$$Y_p(k+1 \mid k) = S_x \Delta x(k) + \mathrm{I} y_c(k) + S_u \Delta U(k) \tag{6}$$

where

$$S_x = \begin{bmatrix} A & A^2 + A & \ldots & \sum_{i=1}^{p} A^i \end{bmatrix}^{\mathrm{T}},$$

$$\mathrm{I} = \begin{bmatrix} I_{2*2} & I_{2*2} & \ldots & I_{2*2} \end{bmatrix}^T,$$

$$S_u = \begin{bmatrix} B & 0 & 0 & \cdots & 0 \\ \sum_{i=1}^{2} A^{i-1}B & B & 0 & \cdots & 0 \\ \vdots & \vdots & \vdots & \cdots & \vdots \\ \sum_{i=1}^{m} A^{i-1}B & \sum_{i=1}^{m-1} A^{i-1}B & \cdots & \cdots & B \\ \vdots & \vdots & \vdots & \cdots & \vdots \\ \sum_{i=1}^{p} A^{i-1}B & \sum_{i=1}^{p-1} A^{i-1}B & \cdots & \cdots & \sum_{i=1}^{p-m+1} A^{i-1}B \end{bmatrix}_{(2*p)\times(2*m)}.$$

Based on the above prediction results, the following function is optimized:

$$J = \left\| \Gamma_y (Y_p(k+1 \mid k) - R(k+1)) \right\|^2 + \left\| \Gamma_u \Delta U(k) \right\|^2 \tag{7}$$

where $\Gamma_y = diag\,(\Gamma_{y,1}, \Gamma_{y,2}, \cdots \Gamma_{y,p})$ is the deviation penalty coefficient matrix;

$\Gamma_u = diag\,(\Gamma_{u,1}, \Gamma_{u,2}, \cdots \Gamma_{u,m})$ is the control increment penalty coefficient matrix;

$\mathrm{R}(k+1) = \begin{bmatrix} r(k+1) & r(k+2) & \ldots & r(k+p) \end{bmatrix}^T$ is the desired response in the prediction time domain, which represents the desired yaw rate and slip angle. Suppose that the desired yaw rate and slip angle responses are constant and it is equal to the current

value $r(k+i)=r(k)$. Solve the equation $\frac{\partial \mathrm{J}}{\partial \Delta U}=0$ and get the optimum control sequence as follow:

$$\Delta U^{*}(k)=(S_u^T\Gamma_y^T\Gamma_y S_u+\Gamma_u^T\Gamma_u)^{-1}S_u^T\Gamma_y^T\Gamma_y E_p(k+1|k) \quad (8)$$

The control deviation (9) is calculated on line:

$$E_p(k+1|k)=R(k+1)-S_x\Delta x(k)-\mathrm{I}y_c(k) \quad (9)$$

According to the model predictive control principle, suppose the response of prediction time domain is constant in the algorithm and make $R(k+1)$ equal to the desired response. The better optimization results are got by adjusting the penalty coefficient. The penalty coefficients are adopted in this paper as follows:

$\Gamma_{yi}=diag([2000,1200])$, $\Gamma_y=diag(\Gamma_{y,1},\Gamma_{y,2},\cdots\Gamma_{y,p})$

$\Gamma_u=diag([0.001\ 0.03;0.001\ 0.03])$

3.2. Driving Force Allocation Controller

The total driving torque T_{xrep} and yaw moment ΔM calculated in the integrated control layer are ultimately achieved by the driving force distributor in the control allocation layer. Every wheel tire longitudinal driving force F_{xi} is controlled by controlling the motor torque.

$$T_{x1}+T_{x2}+T_{x3}+T_{x4}=T_{xrep} \quad (10)$$

$$\mathrm{F}_{xi}=T_{xi}/r_i, \quad (11)$$

where T_{xi} is the motor output torque. T_{xrep} is the total driving torque calculated by the integrated control layer. r_i is the wheel rolling radius. $i=1,2,3,4$, represents front left wheel, front right wheel, rear left wheel and rear right wheel. The vehicle coordinate system oxyz in [16] is used. The origin of the coordinate system o coincides with the center of gravity (CG) of the vehicle. x-axis is parallel to the ground and points to the front. z-axis points to top through the center of gravity. y-axis points to the left of the driver. Yaw moment ΔM is controlled by the longitudinal driving force allocation. Yaw moment control is expressed by the driving force as follows:

$$\Delta M=B[F_{x1}\quad F_{x2}\quad F_{x3}\quad F_{x4}]^T, F_{xi}\geq 0 \quad (12)$$

where

$$B=\begin{bmatrix} -\frac{w}{2}cos(\delta_f)+a\cdot sin(\delta_f) \\ \frac{w}{2}cos(\delta_f)+a\cdot sin(\delta_f) \\ -\frac{w}{2} \\ \frac{w}{2} \end{bmatrix}^T$$

First, according the yaw moment ΔM and desired yaw rate γ_d to judge the understeer and oversteer by the rules as follows: When $\Delta M>0$ and $\gamma_d>0$, the vehicle in the left understeer condition; When $\Delta M>0$ and $\gamma_d<0$, the vehicle in the right oversteer condition; When $\Delta M<0$ and $\gamma_d>0$, the vehicle in the left oversteer condition. When $\Delta M<0$ and $\gamma_d<0$, the vehicle in the right understeer condition. Then, the driving force allocation is controlled by rules as follows: When the vehicle needs to correct left understeer or right oversteer, each of right side wheels driving torque increases 1/4 yaw moment and each of left side wheels driving torque reduces 1/4 yaw moment. When the vehicle needs to correct left oversteer or right understeer, each of left side wheels drive torque increases 1/4 yaw moment and each of right side wheels driving torque reduces 1/4 yaw moment.

3.3. Active Suspension Controller

Active suspension control changes the front and rear axle cornering stiffness through the allocation and control of the vertical load transfer. When need to increase the vehicle understeer, the front axle load transfer increases and the rear axle load transfer decreased. When need to decrease the vehicle understeer, the front axle load transfer decreases and the rear axle load transfer increased.

Quasi-static equation of the suspension roll dynamics:

$$a_y m_s h=(K_{\varphi f}+K_{\varphi r})\varphi+\Delta F_{sf}w+\Delta F_{sr}w \quad (13)$$

The maximum transfer load of the vehicle in steering process is $a_y m_s h_r/w$. a_y is the lateral acceleration, $K_{\varphi i}$ is the suspension roll angle stiffness, ΔF_{si} is the suspension control force. Suspension control force must be less than the unilateral load when driving in straight-line.

$$\begin{aligned} 0\leq\Delta F_{Sf}\leq F_{z1}/2 \\ 0\leq\Delta F_{Sr}\leq F_{z2}/2 \end{aligned}, \quad (14)$$

where F_{z1} , F_{z2} are the front, rear axle vertical loads; ΔF_{Sf} , ΔF_{Sr} are the front and rear axle suspension control forces. ΔF_S is the suspension control force.

$$\Delta F_S = \Delta F_{Sf} + \Delta F_{Sr} \le a_y m_s h / w \tag{15}$$

$$\max\left(\Delta F_S - \frac{F_{Sr}}{2}, 0\right) \le \Delta F_{Sf} \le \min\left(\frac{F_{Sf}}{2}, \Delta F_S\right) \tag{16}$$

Active suspension controller adopts the PID controller. The error of the actual yaw rate value and the desired yaw rate value is as the control input. The front axle suspension force within the reasonable range is as the control output u . (shown in Fig. 3)

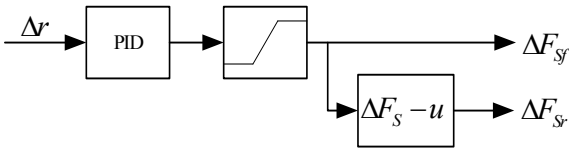

Fig. 3. Suspension controller schematic.

4. Algorithm Verification

In order to verify the validity of the algorithm, the J-turn steering input open-loop test is adopted. J-turn wheel steering input is as shown in Fig. 4. The simulation speed is 80 km/h and the road adhesion coefficient is 0.8. The simulation results as shown in Fig. 5.

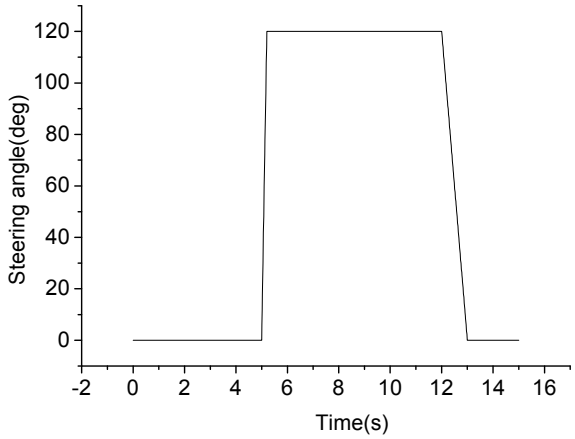

Fig. 4. Steering angle of J-Turn.

It can be seen that the integrated control can better reduce the overshoot and shake in a sharp turn from the simulation results. It makes vehicle track the desired yaw rate and slip angle effectively and the AFS/DYC/AS integrated control is better than the AFS/DYC integrated control, as shown in Fig. 5 (a), Fig. 5 (b). The response of the active steer angle, driving forces are better by the AFS/DYC/AS integrated control compare to the AFS/DYC integrated control, and it can improve the vehicle stability margin by the AFS/DYC/AS integrated control, as shown in Fig. 5 (c), Fig. 5 (d), Fig. 5 (e). Body roll angle is obvious better by AFS/DYC/AS integrated control compare to no control and the AFS/DYC integrated control, which can effectively prevent the roll and improve ride comfort, as shown in Fig. 5 (f). The trend of the active suspension force, active steer angle and driving torque are the same, which reflects the integrated control to achieve the same goal, as shown in Fig. 5 (g).

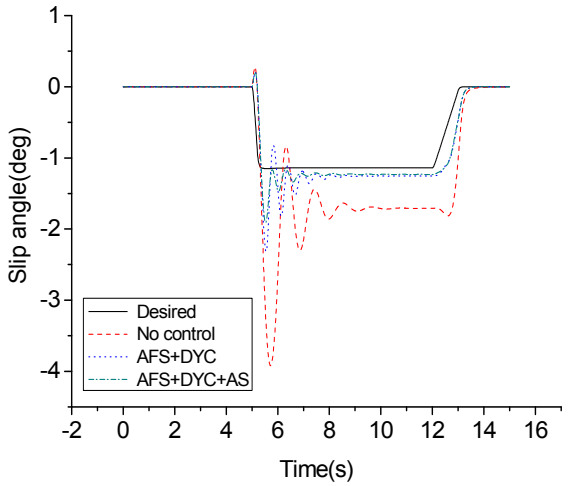

Fig. 5 (a). Simulation results for J-Turn maneuver: slip angle.

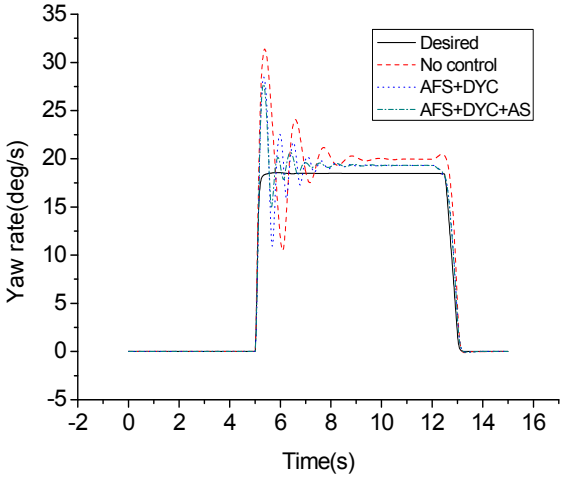

Fig. 5 (b). Simulation results for J-Turn maneuver: yaw rate.

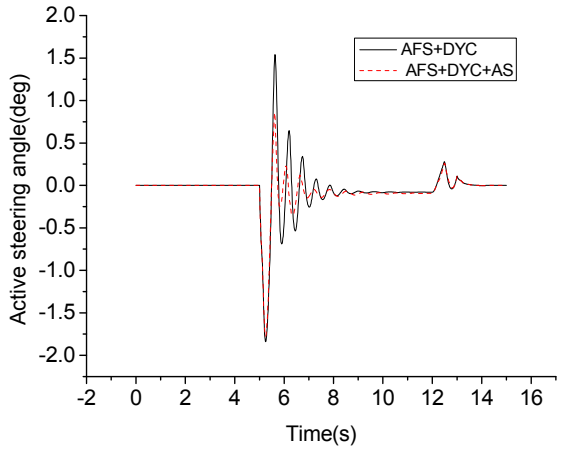

Fig. 5 (c). Simulation results for J-Turn maneuver: active steering angle.

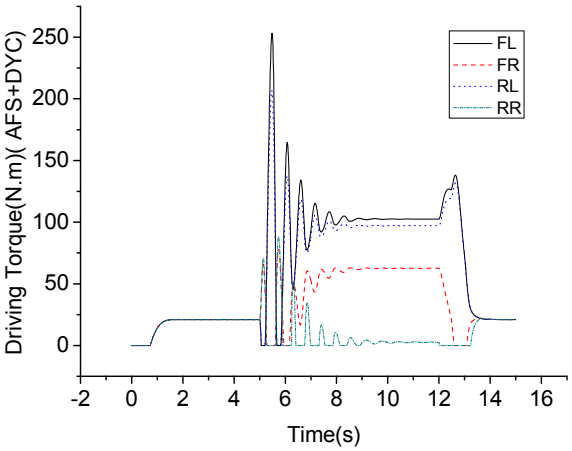

Fig. 5 (d). Simulation results for J-Turn maneuver: driving torque (AFS+DYC).

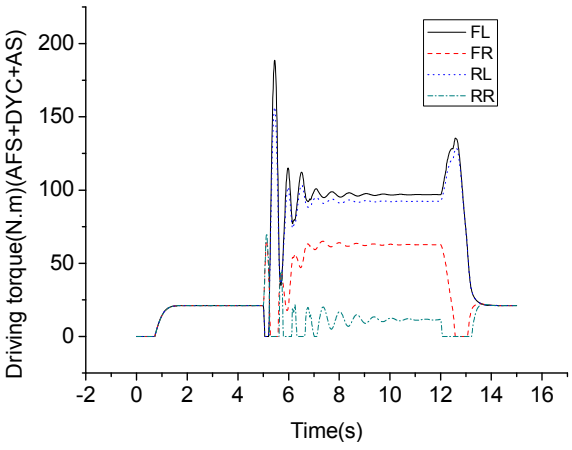

Fig. 5 (e). Simulation results for J-Turn maneuver: driving torque (AFS+DYC+AS)

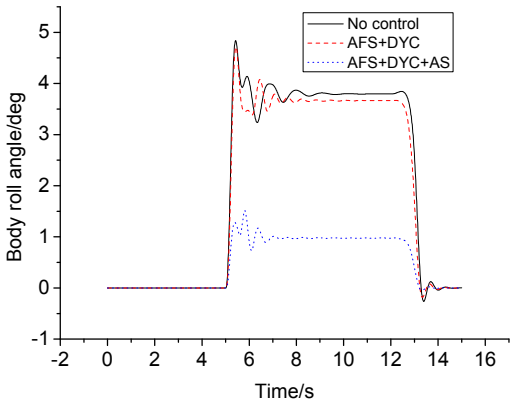

Fig. 5 (f). Simulation results for J-Turn maneuver: body roll angle.

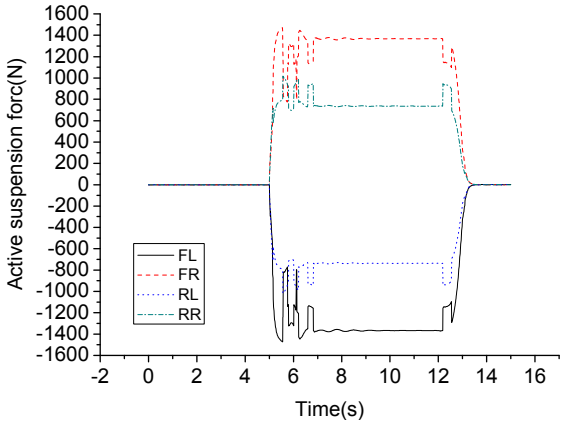

Fig. 5 (g). Simulation results for J-Turn maneuver: active suspension force

5. Conclusion

For four in-wheel motor electric vehicle, the AFS/DYC and AFS/DYC/AS integrated control based on model predictive control theory are studied. The integrated control can improve vehicle stability and active safety effectively. Model predictive control method can make the vehicle slip angle and yaw rate in the ideal range by adjusting the weights of control variable and input variable online. The AFS/DYC/AS integrated control is better than the AFS/DYC integrated control in tracking the desired value and improving the vehicle performance of the stability and safety.

Acknowledgment

This work was supported by National Youth Natural Science Foundation of China (Project No. 51305190), Opened Foundation of State Key Laboratory of Automotive Simulation and Control (Project No. 20111104) and Liaoning University of Technology Foundation (Project No. 201108).

References

[1]. Satoshi Murata, Vehicle dynamics innovation with in-wheel motor, *SAE Paper*, 2011-39-7204.

[2]. Jochen Rauh and Dieter Ammon, System dynamics of electrified vehicles: some facts, thoughts, and challenges, *Vehicle System Dynamics*, Vol. 49, No. 7, July 2011, pp. 1005–1020.

[3]. Michelin's Active Wheel technology in detail (www.motorauthority.com/news/1030025_michelins-active-wheel-technology-in-detail).

[4]. Geng Cong, Mostefai Lotti, Denai Mouloud, Hori Yoichi, Direct yaw-moment control of an in-wheel-motored electric vehicle based on body slip angle fuzzy observer, *IEEE Transactions on Industrial Electronics*, Vol. 56, Issue 5, 2009, pp. 1411-1419.

[5]. Yu Zhuo-Ping, Jiang Wei, Zhang Li-Jun, Torque distribution control for four wheel in wheel motor electric vehicle, *Journal of Tongji University: (Natural Science),* Vol. 36, Issue 8, 2008, pp. 1115-1119. (in Chinese).

[6]. Zou Gangcai, Luo Yu-Gong, Li Ke-Qiang, Tire longitudinal force optimization distribution for independent 4WD EV, *Journal of Tsinghua University (Sci &Tch)*, Vol. 49, Issue 5, 2009, pp. 719-722, 727.

[7]. Zheng Hong-Yu, Research on road feeling and active steering control strategy for vehicle steer-by-wire system, Dissertation, *Jilin University*, Changchun, 2009. (in Chinese).

[8]. Masao Nagai, The perspectives of research for enhancing active safety based on advance control technology, *Vehicle System Dynamics*, Vol. 45, Issue 5, 2007, pp. 413–431.

[9]. Xiujian Yang, Zengcai Wang, Weili Peng, Coordinated control of AFS and DYC for vehicle handling and stability based on optimal guaranteed cost theory, *Vehicle System Dynamics*, Vol. 47, Issue 1, 2009, pp. 57–79.

[10]. I. Youn, J. Im, M. Tomizuka, Level and attitude control of the active suspension system with integral and derivative action, *Vehicle System Dynamics*, Vol. 44, Issue 9, 2006, pp. 659-674.

[11]. Jun Wang, Shuiwen Shen, Integrated vehicle ride and roll control via active suspension, *Vehicle System Dynamics*, Vol. 46, Issue 1, 2008, pp. 495-508.

[12]. Daofei Li, Study on integrated vehicle dynamics control based on optimal tire force distribution, *Shanghai Jiao Tong University*, Shanghai, 2008. (in Chinese).

[13]. Rajesh Rajamani, Vehicle dynamics and control, *Springer*, New York, 2006.

[14]. Zong Changfu, Pan Zhao, Hu Dan, Zhen Hongyu, Xu Ying, Dong Yiliang, Information fusion algorithm for vehicle state estimation based on extended Kalman filtering, *Chinese Journal of Mechanical Engineering*, Vol. 45, Issue 10, 2009, pp. 272-277.

[15]. Xi Yu-Geng, Model predictive control, *National Defense Industry Press*, Beijing, 1993. (in Chinese).

[16]. Yu Zhisheng, Automobile theory, *China Machine Press*, 2010. (in Chinese).

2013 Copyright ©, International Frequency Sensor Association (IFSA). All rights reserved.
(http://www.sensorsportal.com)